Daily measurements were examined for consistency and again the EPID and Starcheck performed similarly, with comparable standard deviations, as shown in Table 1.

	Transverse symmetry (%)			Field size X (cm)			Slope (%/mm) / Energy (%)		
Date	EPID	Starcheck	QA3	EPID	Starcheck	QA3	EPID	Starcheck	QA3
15/09/2015	0.5	-	0.04	19.92	-	20.01	0.29	-	107.2
18/09/2015	0.24	-	0.04	19.91	-	20.06	0.29	-	105.9
21/09/2015	0.46	-	0.21	19.91	-	20.01	0.29	-	106.6
23/09/2015	0.36	0.29	0.44	19.91	19.91	20.02	0.29	0.3	106.3
25/09/2015	0.42	0.32	0.33	19.93	19.87	20.05	0.29	0.3	106.6
29/09/2015	0.57	0.33	0.11	19.91	19.94	20.01	0.29	0.3	105.7
08/10/2015	0.42	0.34	0.09	19.91	19.92	20.24	0.29	0.3	104.7
12/10/2015	0.42	0.37	0.09	19.91	19.93	20.24	0.29	0.3	105.4
Std Deviation	0.097	0.029	0.147	0.007	0.027	0.101	0.000	0.000	0.791

Table 1 – Table showing the daily measurements and calculated standard deviations for all three devices taken for Symmetry, Fields size and Energy.

Conclusion: Our results show that for FFF QA measurements such as field size and symmetry, using the EPID is a viable alternative to other QA devices. The EPID performs particularly well on geometric measurements, as it is able to detect small changes in positon (~1mm) with good consistency. This is to be expected due to its high resolution when compared to the other QA devices used (EPID 0.34mm, Starcheck 3mm, QA3 5mm). Therefore the EPID could potentially be used for a wider range of QC measurements with a focus on geometric accuracy, such as MLC positional QA.

References [1] Fogliata, A., Garcia, R., et Al (2012). Definition of parameters for quality assurance of flattening filter free (FFF) photon beams in radiation therapy. *Med. Phys.*, 39(10), p.6455.

PO-0817

Characteristics and performance of the first commercial MLC for a robotic delivery system

P. Prins[1], C. Fürweger[2], H. Coskan[1], J.P.A. Marijnissen[1], B.J.M. Heijmen[1]
[1]*Erasmus Medical Center Cancer Institute, Department of Radiation Oncology, Rotterdam, The Netherlands*
[2]*European Cyberknife Center, Munich, Germany*

Purpose or Objective: To assess characteristics and performance of the "InciseTM" MLC (41 leaf pairs, 2.5mm width, FFF linac) mounted on the robotic SRS/SBRT platform "Cyberknife M6TM" in a pre-clinical 5 months test period and to ensure quality of clinical treatments.

Material and Methods: Beam properties were measured with unshielded diodes and EBT3 film. Bayouth tests for leaf / bank position accuracy were performed in standard (A/P) and clinically relevant non-standard positions, before and after exercising the MLC for 10+ minutes. Total system accuracy was assessed in End-to-End tests. Delivered dose was verified with EBT3 film for exemplary and clinical plans. Stability over time was evaluated in Picket-Fence- and adapted Winston-Lutz-tests (AQA) for different collimator angles.

Results: Penumbrae (80-20%, with 100%=2*dose at inflection point; SAD 80cm; 15mm depth) parallel/perpendicular to leaf motion ranged from 2.7/2.2mm for the smallest (0.76x0.75cm2) to 3.7/3.6mm for larger (8.26x8.25cm2) square fields. MLC penumbrae are slightly wider than penumbrae fixed cones (2.1 to 2.8mm for 5 to 60 mm cones). Interleaf leakage was <0.5%. Average leaf position offsets were ≤0.2mm in 14 standard A/P Bayouth tests and≤0.6mm in 8 non-standard direction tests. Pre-test MLC exercise slightly increased jaggedness (range +/-0.3mm vs. +/-0.5mm) and allowed to identify one malfunctioning leaf motor. Total system accuracy with MLC was 0.39+/-0.06mm in 6 End-to-End tests. Delivered dose showed good agreement with calculated dose (typically Gamma(3%,3mm)<1 for >95% of pixels with D > 0.1 Dmax). Picket-Fence and AQA showed no adverse trends (> 1 yr).

Conclusion: The InciseTM MLC for CyberKnife M6TM displays high mechanical stability and accurate dose delivery. The specific CK geometry and performance after exercise demand dedicated QA measures.

PO-0818

Multicentre small field measurements using a new plastic scintillator detector

M. Pasquino[1], S. Russo[2], P. Mancosu[3], E. Villaggi[4], G. Loi[5], R. Miceli[6], G.H. Raza[7], A. Vaiano[8], M.D. Falco[9], E. Moretti[10], F.R. Giglioli[11], R. Nigro[12], C. Talamonti[13], G. Pastore[14], E. Menghi[15], F. Palleri[16], S. Clemente[17], C. Marino[18], G. Borzi[19], V. Ardu[20], S. Linsalata[21], A. Mameli[22], V. D'Alesio[23], F. Vittorini[24], M. Stasi[1]
[1]*A. O. Ordine Mauriziano di Torino - Ospedale Mauriziano Umberto I, Medical Physics, Torino, Italy*
[2]*Azienda Sanitaria di Firenze, Medical Physics, Firenze, Italy*
[3]*Humanitas, Radiotherapy, Milano, Italy*
[4]*AUSL Piacenza, Medical Physics, Piacenza, Italy*
[5]*AOU Maggiore delle Carità, Medical Physics, Novara, Italy*
[6]*AOU Tor Vergata, Medical Physics, Roma, Italy*
[7]*Ospedale San Pietro Fatebenefratelli, Medical Physics, Roma, Italy*
[8]*USL 3, Medical Physics, Pistoia, Italy*
[9]*Policlinico SS. Annunziata, Radiotherapy, Chieti, Italy*
[10]*AOU "Santa Maria della Misericordia", Medical Physics, Udine, Italy*
[11]*AOU Città della Salute e della Scienza, Medical Physics, Torino, Italy*
[12]*O.G.P. S.Camillo de Lellis, Radiotherapy, Rieti, Italy*
[13]*AUO Careggi, Medical Physics, Firenze, Italy*
[14]*Ecomedica, Radiotherapy, Empoli, Italy*
[15]*I.R.S.T., Medical Physics, Meldola, Italy*
[16]*AO Parma, Medical Physics, Parma, Italy*
[17]*IRCCS CROB, Medical Physics, Rionero in Vulture, Italy*
[18]*Humanitas, Medical Physics, Catania, Italy*
[19]*Centro REM Radioterapia, Radiotherapy, Catania, Italy*
[20]*Policlinico San Donato, Radiotherapy, San Donato M.se, Italy*
[21]*USL Lucca, Medical Physics, Lucca, Italy*
[22]*Campus Biomedico, Radiotherapy, Roma, Italy*
[23]*Malzoni Radiosurgery Center, Radiotherapy, Agropoli, Italy*
[24]*ASL1 Abruzzo, Medical Physics, L'Aquila, Italy*

Purpose or Objective: Small field dosimetry standardization is fundamental to ensure that different institutions deliver comparable and consistent radiation doses to their patients. The current study presents a multicenter small field evaluation including: Tissue Phantom Ratio (TPR), dose profiles FWHM and penumbra, and output factors (OF), for the two major linear accelerator manufacturers and different X-ray energies.

Material and Methods: The project enrolled 31 Italian centers, 15 equipped with Elekta Linacs and 16 with Varian Linacs. Each center performed TPR measurement, in-plane and cross-plane dose profile of 0.8x0.8cm2 field and OFs measurements for field sizes ranging from 0.6x0.6 cm2 to 10x10 cm2 defined by both secondary jaws and MLC. Set-up conditions were: 10cm depth in water phantom at SSD 90cm. Measurements were performed using the new Exradin W1 plastic scintillator detector (Standard Imaging). The two canals SuperMAX electrometer (Standard Imaging) to automatically correct for Cherenkov radiation was used. Two identical W1 were used to speed up the data collection.

Results: The analysis included 13 Varian and 13 Elekta centers; 7 centers were excluded due to a condenser problem in an electrometer. As reported in Table 1 for the two most representative linac models, TPR measurements showed standard deviations (SD)=0.6%; penumbra values of dose profiles showed SD=0.5mm, while FWHM measurements showed a greater variability. As illustrated in Figure 1, OF measurements showed standard deviations within 1.5% for field size greater than 2x2 cm2; for field size less than 2x2 cm2 measurements' variability increases with decreasing field size. OF values show no dependence from the effective field size.

Table 1. TPR, FWHM and penumbra values measured with W1 PSD for the two most representative linacs of the multicenter study

Manufacturer	Model	Energy	TPR	FWHM (mm)		Penumbra (mm)	
Varian	Clinac 2100	6	0.670±0.003	8.1±0.4	7.9±0.5	2.3±0.4	2.3±0.2
Elekta	Agility	6	0.688±0.004	9.3±0.4	7.9±0.5	4.2±0.4	2.7±0.2

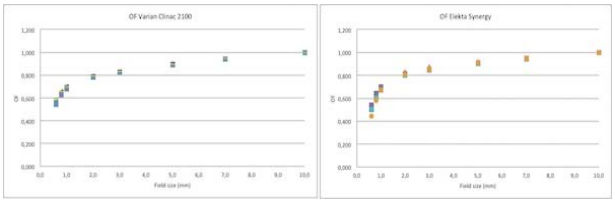

Fig. 1. OF values measured with W1 PSD for the two most representative linacs of the multicenter study

Conclusion: High TPR and penumbra values consistency were obrained over the centers. FWHM and OF showed greater variability, also considering Linac with the same model of the head. Measurements confirm W1 PSD as a good candidate for small field clinical radiation dosimetry in advanced radiation therapy techniques.

PO-0819

Analysis of liquid embolic agents on flattening filter free dose deposition with Monte Carlo method

D. Akcay[1]
[1]*Dokuz Eylul University Medical Faculty, Radiation Oncology, IZMIR, Turkey*

Purpose or Objective: Brain Arteriovenous mal-formation (AVM), in some cases, is treated with Onyx34 liquid embolic system (LES) containing tantalum. Moreover, stereotactic radiosurgery (SRS) may be required when total obliteration is not achieved after embolization. Presence of tantalum in radiation field not only generates artefacts in computed tomography (CT) images but also it could arise dose distribution perturbations. Goal in this study was to analyze the perturbation effect of Onyx34 in flattening filter free (FFF) photon beams using GAMOS Monte Carlo (MC). Artefact cause analysis was also included in the study.

Material and Methods: GAMOS simulations for 6 FFF and 10 FFF photons were done in three different conditions: a) depth dose simulations in a water phantom containing 2x2x2 cm3 Onyx34 (inc. %35wt/vol Ta) medium at 5 cm depth, b) depth dose simulations in the same condition with compact bone instead of Onyx34, c) simulations in homogenous water phantom. Dose and photon flux scorers were used at central beam axis with 5x5x2 mm3 grid sizes. For comparison purposes, photon fluxes were also scored with broad photon beam with single photon energy of 80 keV. All of MC calculations were done with 1.5% and 0.5% statistical noise respectively.

Results: In 80 keV photon simulations, photon flux decreased around 50% at post Onyx34 region relative to homogeneous water simulations. However, for compact bone falloff was around 10% at the same geometry. Also, there was a remarkable flux reduction in pre-Onyx34 region which is not as much as post Onyx34 region. For both 6 and 10 FFF photon beams, around 5% of decrease was seen in photon flux and depth dose after Onyx34 and compact bone inhomogeneties . Pre-Onyx34 region doses were increased by 15% for 6 FFF and 10% for 10 FFF.

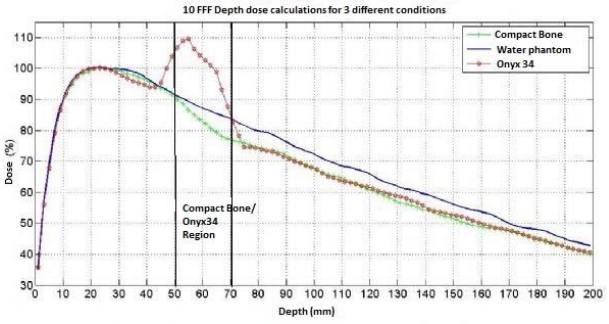

Conclusion: Photon flux calculations for 80 keV beam, showed a considerable photon attenuation and lateral scattering due to presence of Onyx34. As a result, photon starvation causes black-white streak artefacts in CT images. In conclusion, in AVM SRS planning the presence of LES can be taken into account by defining high density artefact region as a compact bone. However in vicinity of critical structures, the possible dose peaks must be considered at pre-Onyx regions which might not be calculated in treatment planning systems.

PO-0820

Volumetric quality assurance of RapidArc plans for multiple intracranial targets using gel dosimetry

N. Khater[1], C. El Khoury[1], M. Sarraf[2], J. Barouky[1], D. Nehme Nasr[1], F. Azoury[1], T. Felefly[1], R. Sayah[1], N. Farah[1], S. Achkar[1], E. Nasr[1]
[1]*Hotel Dieu de France - University of Saint Joseph, Radiation Oncology, Achrafieh, Lebanon*
[2]*Clinatec-Cea-Grenoble, University of Joseph Fourier - University of Saint Joseph, Grenoble, France*

Purpose or Objective: Given the unlimited spatial arrangements of multiple intracranial tumors, an evaluation of a planar sampling for end-to-end test is insufficient as it could provide no information about one or more tumors. Hence, a volumetric approach is needed. Here, we evaluate polymer gel dosimetry for three-dimensional (3D) patient-specific quality assurance (QA) in multiple brain lesions stereotactic radiosurgery (SRS) plans using volumetric modulated arc therapy (VMAT) technique.

Material and Methods: End-to-end test using polymer gel dosimeters was performed for an intracranial SRS case involving two lesions treated with VMAT – single isocenter approach. The following was performed: (1) BANG-3 polymer gel was prepared for two opaque spherical glass phantoms, one for patient plan QA and one for calibration; (2) the patient plan was delivered to the patient phantom and a simple non-modulated plan with predetermined doses was given to the calibration phantom; (3) 1.5T MRI was performed on both phantoms; (4) an in-house program was used to determine the relaxation rate maps (R2) from proton density and T2-weighted images; (5) CT scans were acquired with markers triangulating the isocenter of irradiation setups; (6) CTs were imported into Eclipse treatment planning system for dose computation in corresponding gel phantoms; (7) CTs and MRs were registered in Eclipse and registration transformations used to resample the R2 maps in corresponding CT positions using MATLAB. Then, data analysis was performed using an in-house visual-C++ code which took as input all 3D images, 3D dose, patients' structures exported from Eclipse and performed the following: (8) A calibration was extracted from the calibration gel and used in the patient gel QA; (9) the patients' structures were registered with the patients' gel using CT isocenter marks on the gel phantom and through the isocenter on the patients' plan; and (10) compared measured versus planned 3D isodose, dose volume histogram (DVH) analyses, and multi-slice 2D gamma evaluation.

Results: The measured isodose lines and surfaces were well visualized and qualitatively reproduced the calculated dose distribution (Figure 1). Gamma analysis between the dose matrices were carried out using gamma criteria 3% 3mm and 5% 5mm, % dose difference – distance to agreement combination within the volume enclosed by the 50% and the 80% isodose surface, respectively. Representative transverse slices yielded gamma pass rates of greater than 90%. Measured and planned DVH analyses showed agreement for planning target volume and organs at risk.